Theoretical Investigation of the Mechanisms of Reaction of NCN with NO and NS

Hsin-Tsung Chen and Jia-Jen Ho*

Department of Chemistry, National Taiwan Normal University, 88, Section 4, Tingchow Road, Taipei, Taiwan 117

Received: October 29, 2004; In Final Form: December 31, 2004

Quantum-chemical calculations were performed on the mechanisms of reaction of NCN with NO and NS. Possible mechanisms were classified according to four pathways yielding products in the following four possible groups: $N_2O/N_2S + CN$, $N_2 + NCO/NCS$, $N_2 + CNO/CNS$, and $CNN + NO/NS$, labeled in order from **p1**/**p1s** to **p4**/**p4s**. The local structures, transition structures, and potential-energy surfaces with respect to the reaction coordinates are calculated, and the barriers are compared. In the NCN + NO reaction, out of several adduct structures, only the nitroso adduct NCNNO lies lower in energy than the reactants, by 21.89 kcal/mol; that adduct undergoes rapid transformation into the products, in agreement with experimental observation. For the NS counterpart, both thionitroso NCNNS and thiazyl NCNSN adducts have energies much lower than those of the reactants, by 43 and 29 kcal/mol, respectively, and a five-membered-ring NCNNS (having an energy lower than those of the reactants by 36 kcal/mol) acts as a bridge in connecting these two adducts. The net energy barriers leading to product channels other than **p4s** are negative for the NS reaction, whereas those for the NO analogue are all positive. The channel leading to **p1** ($N_2O + CN$) has the lowest energy (3.81 kcal/mol), whereas the channels leading to **p2** ($N_2 + NCO$) and **p2s** ($N_2 + NCS$) are the most exothermic (100.94 and 107.38 kcal/mol, respectively).

Introduction

Nitrogen oxides attract great interest because of their toxic effects as atmospheric pollutants generated through the combustion of fossil fuels. The mechanisms and rate parameters for reactions involving nitrogen compounds have been extensively investigated in relation to such air pollution.[1] The cyanonitrene radical NCN is proposed to be an important intermediate responsible for the formation of "prompt NO" in the modeling of hydrocarbon flames.[2,3] Many authors have performed studies to characterize the NCN radical theoretically[4−9] and experimentally.[10−22] Optical experiments are limited to independent studies of the triplet and singlet manifolds; accordingly, the NCN molecule is a linear symmetric molecule with a triplet ground state $\tilde{X}^3\Sigma^-$. Most theoretical work has been directed to the structures and vibrational frequencies, although in their work on NCN isomers Martin[9] and Lin[23] found a transition state in the isomerization from NCN to CNN with a large energy barrier. Little is known about the mechanism and the gas-phase kinetics of the reactions of NCN, apart from early reports on the insertion of nitrenes into hydrocarbons.[24−27]

The kinetics of the reaction NCN + NO has been investigated[28] by means of fluorescence spectra over the temperature range 298−573 K to measure total rate coefficients and with temporally resolved infrared spectra as a probe to measure possible products. The reaction has a rate coefficient of $k_{(NCN+NO)} = (2.88 \pm 0.2) \times 10^{-13}$ cm^3 molecule^{-1} s^{-1} at 298 K and a small total pressure, ~3 Torr. Only small proportions of N_2O and CO_2 were detected. The rate coefficient depends on both temperature and pressure, indicating that a major product channel involved the formation of an adduct, which usually does not fall apart to $CN + N_2O$ or $N_2 + NCO$ products but is instead collisionally stabilized. The authors proposed several possible reaction channels and presented this thermochemical information:

$$\mathrm{NCN + NO \rightarrow N_2O + CN}$$
(a) $\Delta H_r^\circ = -25.8$ kJ/mol $= -6.17$ kcal/mol
$$\rightarrow \mathrm{N_2 + NCO}$$
(b) $\Delta H_r^\circ = -411.6$ kJ/mol $= -98.47$ kcal/mol
$$\rightarrow \mathrm{N_2 + CNO}$$
(c) $\Delta H_r^\circ = -110.9$ kJ/mol $= -26.53$ kcal/mol
$$\rightarrow \mathrm{CO + N_3}$$
(d) $\Delta H_r^\circ = -239.3$ kJ/mol $= -57.25$ kcal/mol
$$\rightarrow \mathrm{CNN + NO}$$
(e) $\Delta H_r^\circ = 126.4$ kJ/mol $= 30.24$ kcal/mol
$$\rightarrow \mathrm{NCNNO(f)}$$

Their results indicated that both channels a and b were active to a minor extent, whereas adduct formation in channel f was a major, and possibly dominant product, channel. No refined quantum-chemical calculation on the title reaction is reported so far, but Wang et al.[29] reported an experimental and computational (BAC-MP4) study of the reverse reaction:

$$\mathrm{CN + N_2O \rightarrow [NC\cdots NNO]^{\ddagger} \rightarrow NCNNO \rightarrow [NCN\cdots NO]^{\ddagger} \rightarrow NCN + NO} \quad \text{(g)}$$

$$\mathrm{CN + N_2O \rightarrow [NNO\cdots CN]^{\ddagger} \rightarrow N_2 + NCO} \quad \text{(h)}$$

The rate for $CN + N_2O$ was measurable above 500 K, with a least-squares average rate constant of $k = 10^{-11.8\pm0.4} \exp(-3560 \pm 181/T)$ cm^3/s. On the basis of the results of their calculation, these authors concluded that the reaction took place via a NCNNO adduct, which dissociated into the final products

* Corresponding author. Phone: (886)-2-29309085. Fax: (886)-2-29324249. E-mail: jjh@cc.ntnu.edu.tw.

10.1021/jp045060w CCC: $30.25
Published on Web 02/26/2005

TABLE 1: C−N Bond Length and Singlet−Triplet Energy Gap of the NCN Molecule Calculated at Various Levels of Theory and Some Experimental Data Available from the Literature

levels of theory and experiment	C−N bond length (Å)	singlet−triplet splitting[a] (eV)
B3LYP/6-31G	1.247	
B3LYP/6-31+G*	1.234	1.46
B3LYP/6-311++G**	1.226	
CCSD(T)/TZ2P	1.233	
CCSD(T)/6-311++G**	1.239	1.36
CCSD(T)/aug-cc-pVDZ//B3LYP/6-31+G*		1.35
CCSD(T)/aug-cc-pVTZ//B3LYP/6-31+G*		1.25
G2M		1.11 (0.88 for CNN molecule)
experiment	1.232[b]	1.01[c] (0.846 ± 0.014 for CNN molecule)[c]

[a] The energy separation between the triplet ground state and the excited singlet electronic state. [b] Reference 35. [c] Reference 36 for NCN and ref 37 for CNN.

NCN + NO, instead of the commonly assumed and highly exothermic products NCO + N_2. In their work, the NCNNO adduct was not directly detected and no spectral information was known. To elucidate the structure of this adduct and to obtain energetic data for possible mechanisms of the title reaction, we conducted calculations with density-functional theory (DFT) and high-level quantum-chemical (G2M) methods.

Method of Calculation

The calculation was performed with the Gaussian-98 program package.[30] Stationary points on the potential-energy hypersurfaces were optimized mainly with density-functional theory, the Becke three-parameter hybrid method, and the Lee−Yang−Parr correlation functional approximation (B3LYP).[31−32] We used basis sets with an increasing accuracy of polarized split-valence and diffuse functions for heavy atoms 6-31+G*. Vibrational analysis was conducted at the same level of theory to characterize the optimized structures as local minima or transition structures. Zero-point energy (ZPE) corrections were incorporated. A calculation of the intrinsic reaction coordinate (IRC)[33] was performed to confirm the connection between the transition structure and the specified intermediates. To obtain more reliable energies, we applied a modified G2M (RCC, MP2) method.[34] The total energy in G2M (RCC, MP2) is calculated as follows:

$$E[\text{G2M(RCC, MP2)}] = E[\text{RCCSD(T)/6-311G(d, p)}] + \Delta E(+3\text{df, 2p}) + \Delta E(\text{HLC}) + \text{ZPE[B3LYP/6-31+G(d)]}$$

Here,

$$\Delta E(+3\text{df, 2p}) = E[\text{MP2/6-311+G(3df, 2p)}] - E[\text{MP2/6-311G(d, p)}]$$

and

$$\Delta E(\text{HLC}) = -0.005\,25n_\alpha - 0.000\,19n_\beta$$

in which HLC represents a small empirical "higher-level correction" and n_α and n_β are the number of electrons with α- and β-spins, respectively; $n_\alpha \geq n_\beta$.

Results and Discussion

In Table 1, we present data for the singlet−triplet energy gap and geometrical parameters of NCN radical calculated at various levels of theory with pertinent experimental data from the literature. The hybrid density-functional B3LYP method with a modest 6-31+G(d) basis set predicts a ground-state triplet for NCN with a C−N bond length of 1.234 Å, to be compared with an experimental value of 1.232 Å,[35] whereas the calculated B3LYP energy for the triplet and singlet gap of NCN, 1.46 eV, substantially overestimates the experimental value for triplet−singlet splitting, 1.01 ± 0.01 eV,[36] shown in Table 1. We performed a single-point energy calculation using the G2M method based on B3LYP geometries to improve this value for NCN to 1.11 eV. Applying the same method (G2M) to a calculation on the CNN molecule, we obtained a reasonable energy, 0.88 eV, to be compared with an experimental value of 0.846 ± 0.014 eV.[37] From our calculation of the heats of formation of the following reactions with the G2M method, our results agree satisfactorily with the predicted values presented between parentheses.

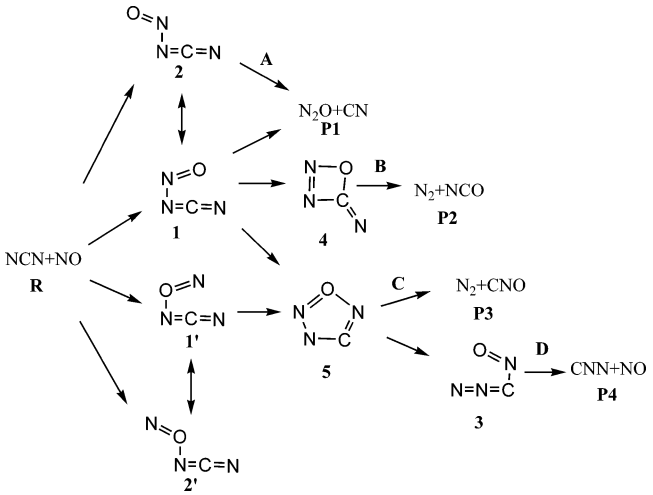

Figure 1. Four possible reaction channels for NCN + NO reactions characterized as **A**, **B**, **C**, and **D**.

$$\text{NCN} + \text{NO} \rightarrow \text{N}_2\text{O} + \text{CN} \qquad \Delta H_r^\circ(\text{G2M}) = -6.02(-6.17)\ \text{kcal/mol}$$

$$\rightarrow \text{N}_2 + \text{NCO} \qquad \Delta H_r^\circ(\text{G2M}) = -100.94(-98.47)\ \text{kcal/mol}$$

$$\rightarrow \text{N}_2 + \text{CNO} \qquad \Delta H_r^\circ(\text{G2M}) = -38.70(-26.53)\ \text{kcal/mol}$$

$$\rightarrow \text{CNN} + \text{NO} \qquad \Delta H_r^\circ(\text{G2M}) = -29.10(-30.24)\ \text{kcal/mol}$$

For this reason, we chose the G2M method to make an energetic calculation for all possible processes in the reaction system NCN + NX with X = O, S.

Reaction NCN + NO. We classified the investigated reaction pathways into four pathways, **A**−**D**, corresponding to products in four groups, as shown in Figure 1. The various intermediates of the reaction are labeled **1**−**5**; the possible products—N_2O + CN, N_2 + NCO, N_2 + CNO, CNN + NO—are labeled in the same order from **p1** to **p4**. $\mathbf{TS}_{i-j}$ denotes transition species related to two intermediates located at local minima ***i*** and ***j***. The geometrical parameters and structures at the local minima calculated at the B3LYP level are drawn in Figure 2, with the transition structures in Figure 3. The potential-energy surfaces (PES) for all possible processes of the reaction calculated at the G2M level are depicted in Figure 4. The calculated ground

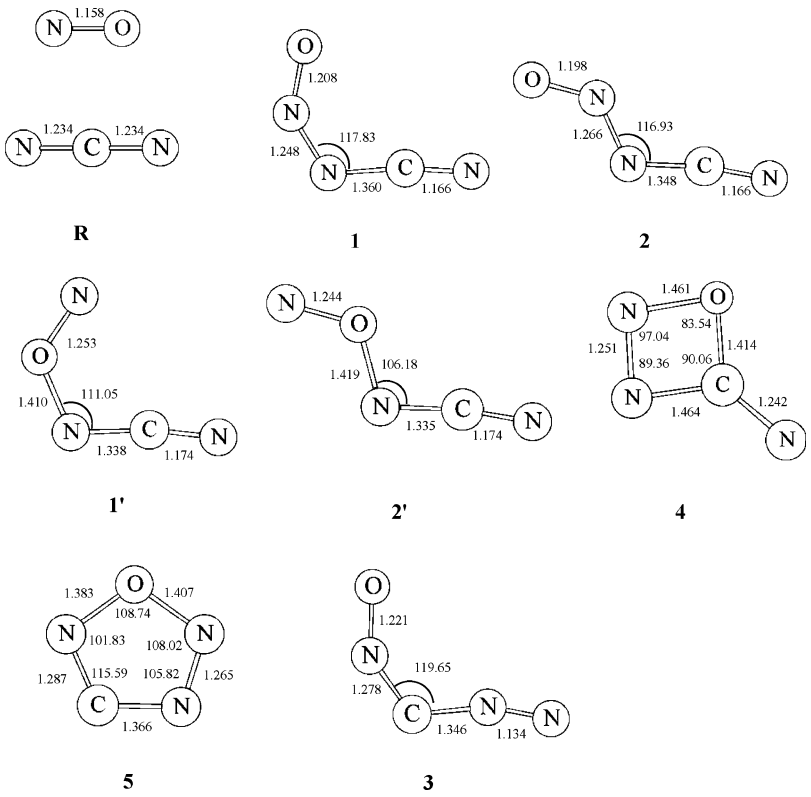

Figure 2. Optimized geometries of the possible intermediates on the potential-energy surfaces of the NCN + NO reaction calculated at the B3LYP/6-31+G* level. Bond lengths are given in angstroms and angles in degrees.

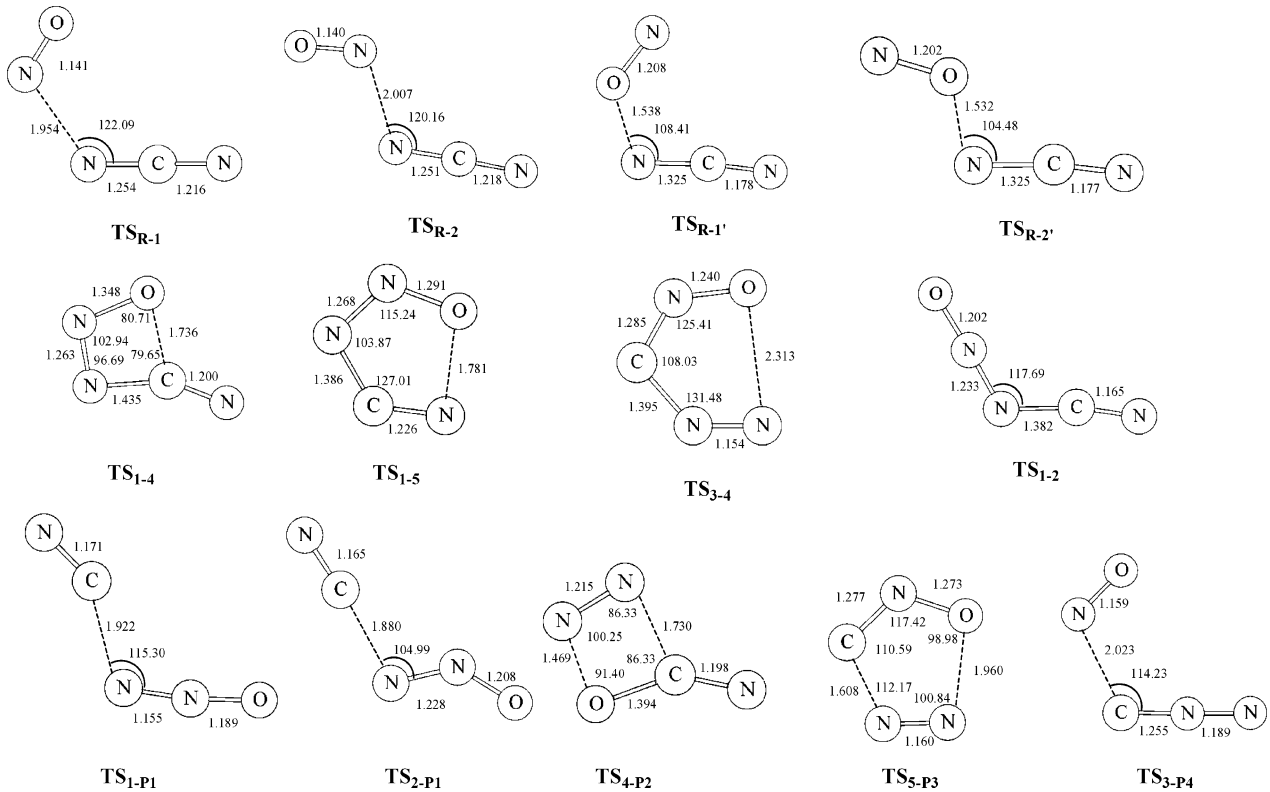

Figure 3. Optimized geometries of the transition structures (**TS**$_{i-j}$) on the potential-energy surfaces of the NCN + NO reaction calculated at the B3LYP/6-31+G* level. Bond lengths are given in angstroms and angles in degrees.

electronic energies and the relative energies of all possible intermediates, transition structures, and products with respect to the reactants, NCN + NO, are listed in Table 2. Two unlikely occurring pathways have exceptional large energy barriers in taking the oxygen atom of NO to bind to a nitrogen of NCN, in forming *cis*- and *trans*-NCNON adducts (**1′** and **2′**), with barrier heights of 39.44 and 39.18 kcal/mol, respectively. Formation of the N−N bond in forming *cis*- and *trans*-NCNNO adducts (**1** and **2**) on taking the nitrogen atom of NO to bind to a nitrogen of NCN requires surmounting only much smaller

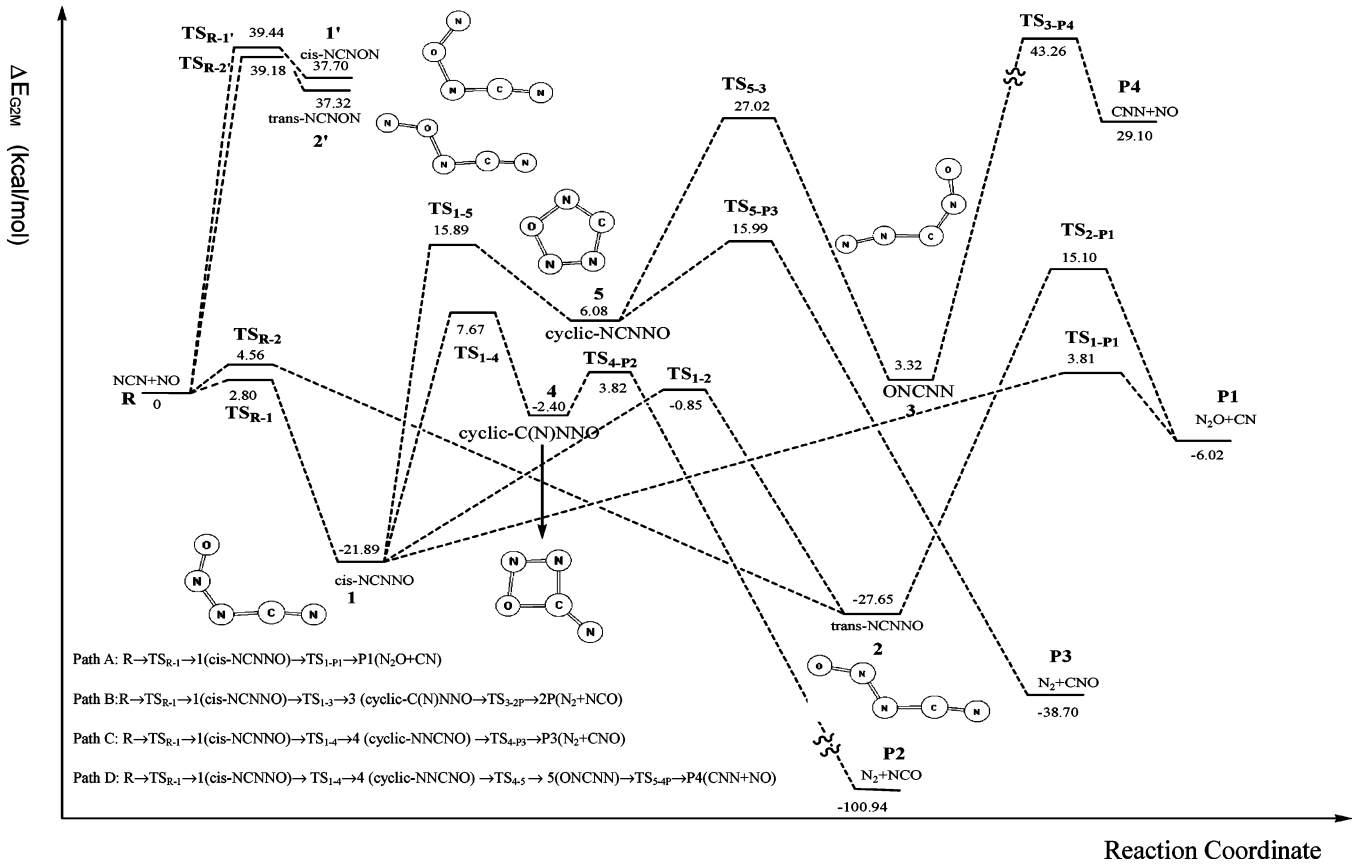

Figure 4. Potential-energy surfaces leading to four possible product channels of the NCN + NO reaction calculated at the G2M level with ZPE correction.

barriers, 2.80 and 4.56 kcal/mol, respectively. For the transition structures of these two adducts, NCNON and NCNNO, the length of bond N···O in the former is ∼1.53 Å, near the local intermediate structure of NCNON (**2′**), 1.419 Å, whereas the N···N distance in transition structure NCNNO is ∼1.95 Å, near that in the reactant intermediate NCN···NO, 2 Å. These phenomena follow Hammond's postulate adequately. The preference for the formation of NCNNO rather than NCNON is explicable with the Fukui function described in a following section. The NCNNO adduct has two isomers, *cis*-NCNNO (**1**) and *trans*-NCNNO (**2**), of which the energies calculated at the G2M level are respectively 21.89 and 27.65 kcal/mol more stable than those of the reactants. Although the trans isomer is more stable than the cis one by ∼5.78 kcal/mol, the energy barrier to form the trans isomer is greater by 1.76 kcal/mol (**TS$_{R-2}$**, 4.56; **TS$_{R-1}$**, 2.80 kcal/mol). Furthermore, the energy barrier of **p1** product formation (N_2O + CN) via *trans*-NCNNO → **TS$_{2-p1}$** → **p1** is greater by 11.29 kcal/mol than that via *cis*-NCNNO → **TS$_{2-p1}$** → **p1**. Therefore, for the formation of **p1** product, the process via *cis*-NCNNO is expected to be more efficient. *trans*-NCNNO might be obtained also from *cis*-NCNNO upon passing through barrier **TS$_{1-2}$**, ∼21 kcal/mol. No product channels other than **p1** are attainable by *trans*-NCNNO, but several other product channels are correlated to the cis counterpart. *cis*-NCNNO can form two cyclic intermediates: four-membered-ring **4** and five-membered-ring **5**, with the former being more stable than the latter by ∼8.5 kcal/mol. The energy barrier to form **4** via transition structure **TS$_{1-4}$** is smaller than that to form **5** via **TS$_{1-5}$** by ∼8.22 kcal/mol. The four-membered-ring intermediate is less stable than *cis*-NCNNO by 19.94 kcal/mol, but it can form **p2** product (N_2 + NCO, thermochemically most stable, −100.94 kcal/mol relative to the reactants) readily upon surmounting the 6.22 kcal/mol barrier (**TS$_{4-p2}$**). Although the five-membered-ring intermediate **5** is less stable than *cis*-NCNNO by 27.97 kcal/mol, it can form a stable **p3** product, N_2 + CNO, −38.70 kcal/mol relative to the reactants, via **TS$_{5-p3}$** by breaking two single bonds, N═C—N and N═N—O, with an energy barrier of 9.91 kcal/mol. Otherwise, it might pass through another higher barrier, **TS$_{5-3}$**, with a barrier height of 20.94 kcal/mol, by breaking another single bond, C═N—O, to form an unstable linear intermediate **3**, 3.32 kcal/mol higher than the reactants, then surmount a large barrier, ∼40 kcal/mol, via **TS$_{3-p4}$** to form a thermochemically unstable **p4** product, CNN + NO, 29.10 kcal/mol higher than the reactants; this channel is the only endothermic one, as all other channels are highly exothermic, especially **B**. As shown in Figure 4, our calculated results indicate that both channels **A** and **B** are two major possible channels of the title reaction and that they compete with each other. As the net barrier height for channel **A** to produce **p1** via **TS$_{1-p1}$** located 3.81 kcal/mol above the reactants is smaller than that for channel **B** to produce **p2** via **TS$_{1-4}$**, 7.67 kcal/mol above the reactants, channel **A** might be considered kinetically the most likely process for the reaction. **p2** is nevertheless the most stable product, being 94.92 kcal/mol lower than **p1**; thus, channel **B** leading to **p2** can be considered the thermochemically preferable process for the reaction. A complication in this system is the involvement of the primary product as the reactant, as NCO, which might also possibly react further with NO, in these secondary reactions:

$$NCO + NO \rightarrow N_2O + CO \quad (E)$$

$$\rightarrow CO_2 + N_2 \quad (F)$$

These reactions have no barrier, and the branching ratio is known: $\varphi_{(E)} = 0.44$ and $\varphi_{(F)} = 0.56$ at 298K studied by Lin et

TABLE 2: Total (au) and Relative Energies (kcal/mol) of the Reactant, Intermediates, Transition States, and Products for NCN with NO Calculated at Different Levels of Theory Based on B3LYP/6-31+G* optimized geometries

	energies						
species	ZPE[a]	B3LYP/6-31+G(d)[b]	MP2/6-311G(d, p)[b]	MP2/6-311+G(3df, 2p)[b]	CCSD(T)/6-311G(d, p)[b]	G2M[b]	G2M[c]
NCN+NO (**R**)	0.012 936	−277.381 053	−276.716 678	−276.871 341	−276.808 206	−277.037 543	0
cis-NCNNO (**1**)	0.019 428	−277.412 543	−276.753 724	−276.919 498	−276.833 375	−277.072 392	−21.89
trans-NCNNO (**2**)	0.019 387	−277.423 489	−276.759 801	−276.925 747	−276.842 369	−277.081 599	−27.65
cis-NCNON (**1′**)	0.015 992	−277.324 583	−276.647 162	−276.809 559	−276.738 390	−276.977 466	37.70
trans-NCNON (**2′**)	0.015 844	−277.327 473	−276.649 635	−276.810 852	−276.740 033	−276.978 076	37.32
cyclic NN(N)CO (**3**)	0.018 369	−277.370 585	−276.727 056	−276.897 702	−276.796 425	−277.041 372	−2.40
cyclic NCNNO (**4**)	0.020 019	−277.361 461	−276.693 795	−276.863 841	−276.785 161	−277.027 858	6.08
NNCNO (**5**)	0.018 350	−277.381 612	−276.699 537	−276.866 767	−276.790 696	−277.032 245	3.32
$\mathbf{TS_{R-1}}$	0.014 878	−277.382 431	−276.691 998	−276.850 247	−276.797 161	−277.033 076	2.80
$\mathbf{TS_{R-2}}$	0.014 806	−277.375 962	−276.698 942	−276.854 305	−276.797 052	−277.030 280	4.56
$\mathbf{TS_{R-1}'}$	0.014 742	−277.324 966	−276.635 264	−276.797 728	−276.734 305	−276.974 698	39.44
$\mathbf{TS_{R-2}'}$	0.014 671	−277.327 997	−276.636 779	−276.797 949	−276.735 930	−276.975 099	39.18
$\mathbf{TS_{1-2}}$	0.017 762	−277.379 886	−276.725 369	−276.892 922	−276.796 442	−277.038 903	−0.85
$\mathbf{TS_{1-3}}$	0.016 597	−277.360 178	−276.698 439	−276.867 840	−276.779 841	−277.025 315	7.67
$\mathbf{TS_{1-4}}$	0.018 209	−277.351 065	−276.651 553	−276.819 236	−276.770 071	−277.012 216	15.89
$\mathbf{TS_{4-5}}$	0.015 715	−277.345 581	−276.630 522	−276.796 626	−276.751 423	−276.994 482	27.02
$\mathbf{TS_{1-P1}}$	0.016 214	−277.364 855	−276.701 816	−276.866 570	−276.790 255	−277.031 465	3.81
$\mathbf{TS_{2-P1}}$	0.016 105	−277.354 504	−276.662 196	−276.825 753	−276.773 365	−277.013 486	15.10
$\mathbf{TS_{3-P2}}$	0.016 085	−277.364 773	−276.683 531	−276.852 494	−276.785 909	−277.031 458	3.82
$\mathbf{TS_{4-P3}}$	0.015 769	−277.349 355	−276.660 968	−276.825 720	−276.770 405	−277.012 058	15.99
$\mathbf{TS_{5-P4}}$	0.014 152	−277.324 703	−276.641 757	−276.806 959	−276.724 885	−276.968 605	43.26
N_2O + CN (**P1**)	0.014 622	−277.370 857	−276.741 821	−276.902 841	−276.808 076	−277.047 143	−6.02
N_2 + NCO (**P2**)	0.015 455	−277.523 485	−276.910 688	−277.069 399	−276.962 474	−277.198 400	−100.94
N_2 + CNO (**P3**)	0.013 515	−277.427 969	−276.804 614	−276.962 847	−276.861 819	−277.099 208	−38.70
CNN + NO (**P4**)	0.012 138	−277.335 952	−276.679 027	−276.835 646	−276.759 083	−276.991 174	29.10

[a] Zero-point energy (au) of the B3LYP/6-31+G(d) level. [b] The energy unit is atomic units. [c] The relative energy with respect to reactants at the G2M level (kcal/mol).

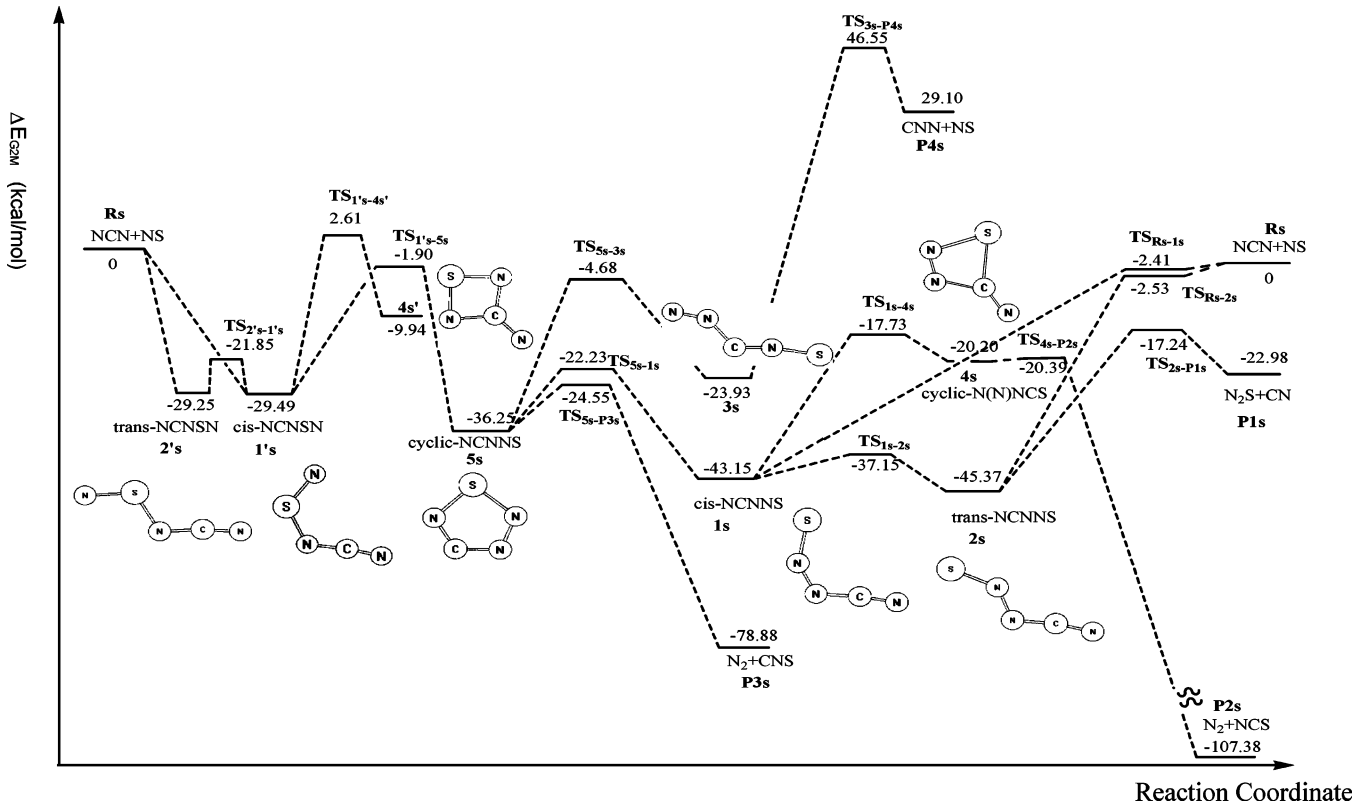

Figure 5. Potential-energy surfaces leading to four possible product channels of the NCN + NS reaction calculated at the G2M level with ZPE correction.

al.[38] and Hershberger et al.[39] For perhaps this reason, CO_2 was detected in experiments on the reaction NCN + NO investigated by Hershberger et al.[28] The other possible products N_3 + CN can result also from a secondary reaction, from NCN + N_2. Our calculation at the G2M level for this secondary reaction showed a large barrier, 74.54 kcal/mol; the reaction NCN + $N_2 \rightarrow N_3$ + CN might thus be negligible. Wang et al.,[29] who studied the reverse reaction of channel **A**, CN + $N_2O \rightarrow$ NCN + NO, concluded that the reaction occurred via a NCNNO adduct, which dissociated into the final products NCN + NO, instead of the commonly assumed and highly exothermic products, NCO + N_2. This argument is consistent with our calculated potential-energy surfaces shown in Figure 4, in which the barrier height to form NCN + NO from *cis*-NCNNO is smaller than that to form NCO + N_2 by ∼5 kcal/mol; the energy of $\mathbf{TS_{1-4}}$ is 7.67 kcal/mol and that of $\mathbf{TS_{R-1}}$ is 2.80 kcal/mol. However, it is still difficult to be conclusive as to what the dominant products (either **p1** or **p2**) should be, since the energy difference (3.86 kcal/mol) between $\mathbf{TS_{1-4}}$ and $\mathbf{TS_{1-p1}}$ is too small (within the calculation uncertainty).

Reaction of NCN + NS. The nitrogen sulfide radical NS, which is isovalent with NO, has been little studied, and few experimental data are available. It was first detected in interstellar clouds with radio frequency techniques[40,41] and then in flames with fluorescence.[42] The NS radical is considered an important intermediate from the interaction of nitrogen- and sulfur-containing species in a flame; it can affect the production of NO_x in exhaust gases. The combustion and atmospheric chemistry of nitric oxide (NO) are extensively studied both experimentally and theoretically,[43−49] but little is known about reactions of its nitrogen sulfide analogue NS. We therefore explain our theoretical mechanistic study for the reaction NS + NCN for comparison with the NO counterpart. Our calculated stable structures, intermediates, and transition structures in the reaction of NCN + NS are similar to those of their NO analogues; their geometrical structures are drawn in Supporting Information Figures 1 and 2. The notation resembles that for NO mechanistic processes, but an "s" is affixed to each number to represent the NS counterpart. The calculated ground electronic energies and relative energies of all possible intermediates, transition structures, and products with respect to reactants NCN + NS are listed in Supporting Information Table 1. The potential-energy surfaces for the NCN + NS reaction calculated at the G2M level are presented in Figure 5. Like NO, either the N atom or the S atom of NS might attack NCN, and each can have both *cis*- and *trans*-NCNNS (thionitroso compounds **1s** and **2s**) and NCNSN (thiazyl compounds **1s′** and **2s′**) adducts. Our calculation shows the formation of both thionitroso and thiazyl adducts to be free of a barrier and extremely exothermic, more than 29 kcal/mol. The thionitroso adducts NCNNS are more exothermic than thiazyl NCNSN by ∼13−16 kcal/mol. This phenomenon is disparate from that of the NO counterpart for which the formation of oxazyl adducts, both *cis*- and *trans*-NCNON, are not only highly endothermic but also associated with large barriers, more than 39 kcal/mol. Because the presence of the S atom can readily accommodate a hypervalent structure, the NS radical can recombine with another radical (R) at both ends, to yield both thionitroso (R−N=S) and thiazyl (R−S≡N) isomers. The relative stability of these two isomers depends on the R substituents. The thiazyl isomer is more stable than the thionitroso isomer upon chlorine substitution (R = Cl), but for R = H, CH_3, CN, NC, and N_3, the order of the relative stability is altered, according to measurements from neutralization−reionization mass spectrometry.[50,51] In our work in which R = NCN, the calculated thionitroso isomer is more stable than the other. Each of the thionitroso, NCN−N=S, and thiazyl, NCN−S≡N, isomers has two conformers (cis and trans), and each is more stable than the reactants NCN + NS by more than 43 kcal/mol for the thionitroso isomer and more than 29 kcal/mol for the thiazyl isomer. Despite our extensive search, we

TABLE 3: Condensed Fukui Functions for the N Atom and C Atom in the NCN Radical and the Two Atoms in NO or NS as well as the Global and Local Softness of the Molecules Calculated at the B3LYP/6-31+G(d) Level

	f^{+} [a]			f^{-} [a]			f^{0} [a]			global softness	local softness[b] (s^0)		
molecule	C	N	O(S)	C	N	O(S)	C	N	O(S)	S[c]	C	N	O(S)
NCN	0.050	0.524		0.214	0.607		0.132	0.566		2.632	0.347	1.489	
NO		0.624	0.376		0.594	0.406		0.609	0.391	2.529		1.540	0.989
NS		0.395	0.605		0.286	0.714		0.341	0.659	3.08		1.050	2.033

[a] The atomic charges are using natural population analysis (NPA). [b] $s^0 = f^0S$. [c] $S = 1/(\mathrm{IE}-A)$; the energy unit is atomic units.

located no **TS** for the migration of the NCN group directly correlating with thionitroso and thiazyl isomers (**1s** and **1s′**); this interconversion can occur via the formation of a five-membered-ring intermediate, cyclic NCNNS (**5s**). Despite also thionitroso being more stable than thiazyl, the formation of the thiazyl isomer is direct, from NCN + NS, free of a barrier, and lacking a transition state. The formation of each thionitroso isomer has a transition state ($\mathbf{TS_{Rs-1s}}$ or $\mathbf{TS_{Rs-2s}}$) with a negative barrier. These results differ from similar mechanistic processes in the reaction NCN + NO, for which the formation of both nitroso and oxazyl isomers requires crossing a positive barrier, with the latter much greater—more than 39 kcal/mol—than the former, ~3−5 kcal/mol. We calculated the Fukui functions[52] and applied hard-and-soft acid-and-base (HSAB) theory to seek possible clues. According to our calculated data in Table 3, the Fukui function 0.609 of the N atom in the NO radical is clearly nearer 0.566 for the N atom in NCN than 0.391 of the O atom, which accounts for the formation of the nitroso compound being preferable to the oxazyl analogue; this argument is inapplicable to the NS case, in which the Fukui function 0.659 of the S atom in the NS radical is nearer that of the N atom in NCN than 0.341 of the N atom. Applying the HSAB theory, we find that the difference of the local softness 2.033 of the S atom in NS and 1.489 of the N atom in NCN is near 1.050 of the N atom in NS and 1.489 of the N atom in NCN, which might account for the almost equally favorable formation of thiazyl and thionitroso compounds. For the *cis*- and *trans*-thiazyl (NCNSN) isomers, cis is more stable than trans by only 0.24 kcal/mol; the barrier height for interconversion between cis and trans is ~7 kcal/mol. However, from our calculated potential-energy surface, shown in Figure 5, the stable five-membered-ring NCNNS (**5s**) formed from the cis conformer (**1s′**) might be the major intermediate correlating with various successive product formations. The transition structure $\mathbf{TS_{1s'-5s}}$ is still lower than the reactants by 1.90 kcal/mol. This exceptional result differs markedly from that in Figure 4 of the NO counterpart, for which the cyclic NCNNO (**5**) is less stable than the reactants by 6.08 kcal/mol, and the transition structure of $\mathbf{TS_{1-5}}$ is much greater by 15.89 kcal/mol (the practicality of this pathway is largely decreased). That the Fukui function 0.659 of the S atom in NS is much nearer 0.566 for the N atom in NCN than 0.391 of the O atom in NO might also account for this result. The pathway from **5s** to **3s** that has a much higher energy barrier, 31.57 kcal/mol, than the corresponding process (**5** to **3**) of the NO counterpart, 20.94 kcal/mol, and the pathway from **5s** to **p3s** for which the barrier is 11.7 kcal/mol compared to that from **5** to **p3** with a smaller barrier, 9.91 kcal/mol, also imply a binding energy of the NN—S bond greater than that for the NN—O bond. Unlike the NO analogue, cyclic **5s** has another reaction channel to form a *cis*-thionitroso compound, with a barrier height of ~14 kcal/mol ($\mathbf{TS_{5s-1s}}$), which acts as a bridge for interconversion between *cis*-thiazyl and *cis*-thionitroso compounds; the barrier height for the reverse channel to form *cis*-thiazyl (**1s′**) is more than 34 kcal/mol, indicating that breaking of the multiple NN bond is inefficient. There is another slim possibility for *cis*-thiazyl (**1s′**) to form a four-membered-ring intermediate (**4s′**) via $\mathbf{TS_{1s'-4s'}}$, with a barrier height greater than 32 kcal/mol, which leads to no connection to other compounds. The *cis*-thionitroso compound (**1s**) can proceed to form other products: First, it can convert into the more stable (by 2.22 kcal/mol) trans conformer (**2s**) via $\mathbf{TS_{1s-2s}}$ (barrier height 6 kcal/mol), which can break either the NC—NNS bond to form **p1s** (N_2S + CN) or the NCN—NS bond to return to the reactants, NCN + NS; the former process has a smaller energy barrier, 28.13 rather than 42.84 kcal/mol. Second, it can surmount the transition state $\mathbf{TS_{1s-4s}}$ (barrier height 25.42 kcal/mol) to form the four-membered-ring intermediate **4s** (lower in energy by 20.20 kcal/mol than the reactants), which then falls apart easily (via a transition structure almost free of barrier, $\mathbf{TS_{4s-p2s}}$) to form the most stable products, **p2s** (N_2 + NCS) and release much energy (more than 87 kcal/mol). Another possibility for the five-membered-ring NCNNS (**5s**) is to break its NN—S bond (via $\mathbf{TS_{5s-3s}}$; barrier height 31.57 kcal/mol) and become the linear structure **3s** (NNCNS, 23.93 kcal/mol lower than the reactants), which is in turn hardly possible to yield product **p4s** (CNN + NS, the only endothermic, 29.10 kcal/mol) via $\mathbf{TS_{3s-p4s}}$ (barrier height 70.48 kcal/mol). Transition structures other than $\mathbf{TS_{3s-p4s}}$ and $\mathbf{TS_{1s'-4s'}}$ are located lower on energy surfaces than the reactants, which imply that most described reaction channels of NCN + NS in Figure 5 can proceed without additional energy thermodynamically (**p2s** is the most exothermic).

Conclusion

With the DFT (B3LYP/6-31+G*) method and the G2M single-point calculation, we calculated possible reaction channels for NCN + NO/NS as well as the energies of local points and transition structures on the potential-energy hypersurfaces. Similar possible products are found in both reactions: they are N_2O/N_2S + CN (**p1**/**p1s**), N_2 + NCO/NCS (**p2**/**p2s**), N_2 + CNO/CNS (**p3**/**p3s**), and CNN + NO/NS (**p4**/**p4s**). The order of magnitudes of the relative energies for these products are also similar, that is, **p2** < **p3** < **p1** < **p4**; **p2s** < **p3s** < **p1s** < **p4s**, but there are several differences between these two reactions: (1) NCN + NS might undergo the formation of a thiazyl adduct NCNSN via a barrier-free exothermic process (~29.5 kcal/mol), whereas the NO counterpart must cross a barrier greater than 39 kcal/mol to form an oxazyl adduct NCNON endothermically (~37.5 kcal/mol). (2) The formation of **4** from *cis*-nitroso compound NCNNO is more stable (by 8.48 kcal/mol) and involves a smaller barrier (by 8.22 kcal/mol) than the formation of **5**, whereas the formation of **4s** from *cis*-thionitroso compound NCNNS is less stable (by 16.05 kcal/mol) and has a greater barrier (by 4.5 kcal/mol) than the formation of **5s**. The larger size of the S atom that stabilizes a larger ring system might account for this effect. (3) **5s** might be a connection between **1s′** and **1s** compounds on the NCN + NS potential-energy surfaces, which is not found for the NO counterpart. Thiazyl adducts are less stable than the thionitroso ones by 13−16 kcal/mol, but both have much smaller energies than the reactants by 29−45 kcal/mol, unlike the NO counterpart for which only the nitroso ones have smaller energies than the

reactants, by 21−27 kcal/mol. From the calculated potential-energy surfaces, we predict that the most efficient product formation in the NCN + NO reaction might be **p1**, but **p2** is thermodynamically favorable. In contrast, products except **p4s** in the NCN + NS reaction reflect their negative net barriers. Among them, **p3s** is kinetically more favorable than **p1s** and **p2s**, but **p2s** is thermodynamically preferable. Analogous to Hershberger's prediction for the reaction NCN + NO that the reaction proceeds primarily through the formation of a NCNNO adduct that undergoes rapid transformation into products, we predict similar processes applicable to the reaction NCN + NS (with the formation of both NCNNS and NCNSN adducts being possible).

Acknowledgment. We thank the National Science Council of the Republic of China (NSC-92-2113-M-003-006) for support of this research and the National Center for High-Performance Computing for providing the Gaussian package and computer time.

Supporting Information Available: Figures showing the optimized geometries of the possible intermediates on the potential surfaces of the NCN + NS reaction calculated at the B3LYP/6-31+G* level and the optimized geometries of the transition structures ($\mathbf{TS}_{is-js}$) of the NCN + NS reaction calculated at the B3LYP/6-31+G* level and table showing the total (au) and relative energies (kcal/mol) of the reactant, intermediates, transition states, and products for the NCN + NS reaction calculated at different levels of theory based on the B3LYP/6-31+G* optimized geometries. This material is available free of charge via the Internet at http://pubs.acs.org.

References and Notes

(1) Miller, J. A.; Bowman, C. T. *Prog. Energy Combust. Sci.* **1989**, *15*, 287.
(2) Moskaleva, L. V.; Lin, M. C. *28th Symp. (Int.) Combust*., in press.
(3) Moskaleva, L. V.; Xia, W.-S.; Lin, M. C. *Chem. Phys. Lett.* **2000**, *331*, 269.
(4) Clifford, P. G.; Wenthold, W. C.; Lineberger, G. A.; Petersson, G. B. Ellison. *J. Phys. Chem. A* **1997**, *101*, 4338.
(5) Berthier, G.; Kurdi, L.; *C. R. Acad. Sci., Paris, Ser. II: Mec., Phys., Chim., Sci. Terre Univers*) **1984**, *299*, 1171.
(6) Suter, H. U.; Huang, M. B.; Engels, B. *J. Chem. Phys.* **1994**, *101*, 7686.
(7) Thomson, C. *J. Chem. Phys.* **1973**, *58*, 841.
(8) Williams, G. R. *Chem. Phys. Lett*. **1974**, *25*, 602.
(9) Martin, J. M. L.; Taylor, P. R.; Francois, J. P.; Gijbels, R. *Chem. Phys. Lett*. **1994**, *226*, 475.
(10) Jennings, K. R.; Linnett, J. W. *Trans. Faraday Soc.* **1960**, *56*, 1737.
(11) Smith, G. P.; Copeland, R. A.; Crosley, D. R. *J. Chem. Phys*. **1989**, *91*, 1987.
(12) Smith, G. P.; Copeland, R. A.; Crosley, D. R. *AIP Conf. Proc.* **1988**, 659.
(13) Kroto, H. W. *J. Chem. Phys*. **1966**, *44*, 831.
(14) Kroto, H. W. *Can. J. Phys.* **1967**, *45*, 1439.
(15) Kroto, H. W.; Morgan, T. F.; Sheena, H. H. *Trans. Faraday Soc*. **1970**, *66*, 2237.
(16) Milligan, D. E.; Jacox, M. E.; Bass, A. M. *J. Chem. Phys*. **1965**, *43*, 3149.
(17) Milligan, D. E.; Jacox, M. E. *J. Chem. Phys*. **1966,** *45*, 1387.
(18) Beaten, S. A.; Ito, Y. J. M. Brown, *J. Mol. Spectrosc*. **1996**, *178*, 99.
(19) Beaton, S. A.; Brown, J. M. *J. Mol. Spectrosc.* **1997**, *183*, 347.
(20) Hensel, K. D.; Brown, J. M. *J. Mol. Spectrosc.* **1996**, *180*, 170.
(21) Wienkoop, M.; Urban, W.; Brown, J. M. *J. Mol. Spectrosc*. **1997**, *185*, 185.
(22) Fluornoy, J. M.; Nelson, L. Y. *Chem. Phys. Lett*. **1970**, *6*, 521.
(23) McNaughton, D.; Metha, G. F.; Tay, R. *Chem. Phys*. **1995**, *198*, 107.
(24) Moskaleva, L. V.; Lin, M. C. *J. Phys. Chem*. *A* **2001**, *105*, 4156.
(25) Barton, D. H. R.; Morgan, L. R. *J. Chem. Soc.* **1962**, 622.
(26) Barton, D. H. R.; Starratt, A. N. *J. Chem. Soc.* **1965**, 2444.
(27) Lwowski, W.; Mattingly, T. W. *Tetrahedron Lett.* **1962**, 277.
(28) Anastassiou, A. G.; Simmons, H. E. *J. Am. Chem. Soc.* **1967**, *89*, 3177.
(29) Baren, R. E.; Hershberger, J. F. *J. Phys. Chem*. *A* **2002**, *106*, 11093.
(30) Wang, N. S.; Yang, D. L.; Lin, M. C. *Int. J. Chem. Kinet.* **1991**, *23*, 151.
(31) Frisch, M. J.; Trucks, G. W.; Schlegel, H. B.; Scuseria, G. E.; Robb, M. A.; Cheeseman, J. R.; Zakrzewski, V. G.; Montgomery, J. A.; Stratmann, R. E., Jr.; Burant, J. C.; Dapprich, S.; Millam, J. M.; Daniels, A. D.; Kudin, K. N.; Strain, M. C.; Farkas, O.; Tomasi, J.; Barone, V.; Cossi, M.; Cammi, R.; Mennucci, B.; Pomelli, C.; Adamo, C.; Clifford, S.; Ochterski, J.; Petersson, G. A.; Ayala, P. Y.; Cui, Q.; Morokuma, K.; Malick, D. K.; Rabuck, A. D.; Raghavachari, K.; Foresman, J. B.; Cioslowski, J.; Ortiz, J. V.; Stefanov, B. B.; Liu, G.; Liashenko, A.; Piskorz, P.; Komaromi, I.; Gomperts, R.; Martin, R. L.; Fox, D. J.; Keith, T.; Al-Laham, M. A.; Peng, C. Y.; Nanayakkara, A.; Gonzalez, C.; Challacombe, M.; Gill, P. M. W.; Johnson, B.; Chen, W.; Wong, M. W.; Andres, J. L.; Gonzalez, C.; Head-Gordon, M.; Replogle, E. S.; Pople, J. A. *Gaussian 98*, revision A.6; Gaussian, Inc.: Pittsburgh, PA, 1998.
(32) (a) Becke, A. D. *J. Chem. Phys*. **1993**, *98*, 5648. (b) Becke, A. D. *J. Chem. Phys.* **1992**, *96*, 2155. (c) Becke, A. D. *J. Chem. Phys.* **1992**, *97*, 9173.
(33) Lee, C.; Yang, W.; Parr, R. G. *Phys. Rev. B* **1988**, *37*, 785.
(34) Gonzalez, C.; Schlegel, H. B. *J. Phys. Chem.* **1989**, *90*, 2154.
(35) Mebel, A. M.; Morokuma, K.; Lin, M. C. *J. Chem. Phys.* **1995**, *103*, 7414.
(36) Clifford, E. P.; Wenthold, P. G.; Lineberger, W. C.; Petersson, G. A.; Ellison, G. B. *J. Phys. Chem*. **1997**, *101*, 4338.
(37) Taylor, T. R.; Bise, R. T.; Asmis, K. R.; Neumark, D. M. *Chem. Phys. Lett*. **1999**, *301*, 413.
(38) Clifford, E. P.; Wenthold, P. G.; Lineberger, W. C.; Petersson, G. A.; Broadus, K. M.; Kass, S. R.; Kato, S.; DePuy, C. H.; Bierbaum, V. M.; Ellison, G. B. *J. Phys. Chem*. *A* **1998**, *102*, 7100.
(39) Zhu, R.; Lin, M. C. *J. Phys. Chem*. *A* **2000**, *104*, 10807.
(40) Cooper, W. F.; Park, J.; Hershberger, J. F. *J. Phys. Chem.* **1993**, *97*, 3283.
(41) Gottlieb, C. A.; Ball, J. A.; Gottlieb, C. J.; Lada, C. J.; Penfield, H. *Astrophys. J.* **1975**, *200*, L151.
(42) Kuiper, T. B. H.; Zuckerman, B.; Kakar, R. K.; Kuiper, E. N. *Astrophys. J.* **1975**, *200*, L147.
(43) Jeffries, J. B.; Crosley, D. R. *Combust. Flame* **1986**, *64*, 55.
(44) Boulart, W.; Nguyen, M. T.; Peeters, J. *J. Phys. Chem.* **1994**, *98*, 8036.
(45) Brownsword, R. A.; Hancock, G. *J. Chem. Soc., Faraday Trans.* **1997**, *93*, 1279.
(46) Peeters, J.; Van Look, H.; Ceursters, B. *J. Phys. Chem.* **1996**, *100*, 15124.
(47) Roggenbuck, J.; Temps, F. *Chem. Phys. L ett.* **1998**, *285*, 422.
(48) Sengupta, D.; Peeters, J.; Nguyen, M. T. *Chem. Phys. Lett.* **1998**, *283*, 91.
(49) Sumathi, R.; Sengupta, D.; Nguyen, M. T. *J. Phys. Chem*. *A* **1998**, *102*, 3175.
(50) Nguyen, M. T.; Sumathi, R.; Sengupta, D.; Peeters, J. *J. Chem. Phys*. **1998**, *230*, 1.
(51) Nguyen, M. T.; Flammang, R. *Chem. Ber*. **1996**, *129*, 1379.
(52) Nguyen, M. T.; Flammang, R. *Chem. Ber*. **1996**, *129*, 1373.
(53) Yang, W.; Mortier, W. J. *J. Am. Chem. Soc.* **1986**, *108*, 5708.